Electronic Supplementary Material (ESI) for Soft Matter.

Supplementary Information

Deformation of phospholipid vesicles in an optical stretcher

Delabre et al.

I. ALIGNMENT OF FIBERS

The alignment of the fibers is checked with a phase contrast microscope. Gross fiber misalignments are easily detectable because trapping is not possible anymore. Interestingly, at small fiber distance, the misalignment can result in a square vesicle as shown in figure S1. This "square" shape clearly shows vesicles are soft objects characterized by a low tension of the vesicle membrane as typical optical forces are only of the order of 10-100 pN. Such misalignment is not desirable in the present context, but might be interesting for vesicle shaping and encapsulation strategies.

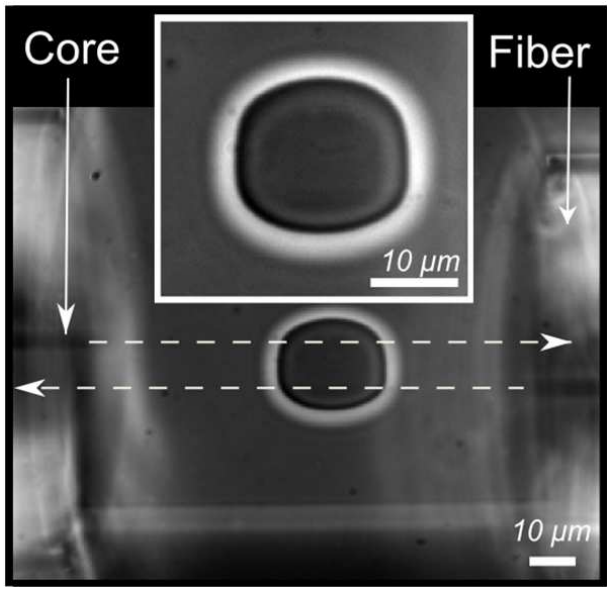

FIG S1: Fiber misalignment observed with a phase contrast microscope. White arrows indicate the fibers axis. The misalignement results here in a square deformation of the vesicle.

II. OPTICAL STRESS

The optical stress was calculating using Ray optics (RO) approximation. The peak stress (i.e. the maximum stress) from RO calculation is also given by the following formula [1]:

$$\sigma_0 = \frac{n_{med}\, I}{c}.(2 - r + r^2)(\frac{n_{scat}}{n_{med}} - 1)$$

where n_{med} is the refractive index of the surrounding medium, n_{scat} is the refractive index of the scatterer (here a vesicle), r is the Fresnel reflexion coefficient for intensity at normal incidence, $I = \frac{2P}{\pi w^2}$ is the laser beam intensity at the interface, P is the power and w the beam waist at the interface of the vesicle along the beam axis. The peak stress is dependent on w but is only very weakly dependent on the radius of the vesicle R since the dependence in R only appears in the beam waist w. However, the optical stress profile is highly dependent on R/w as shown in the polar plots in figure S2 for several

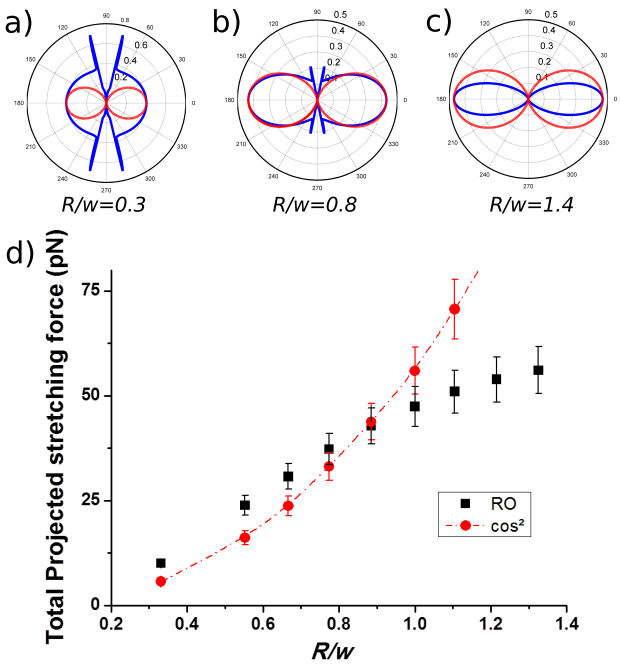

FIG S2: (a-c): In blue: Optical stress profiles in polar coordinates for three ratio R/w : (a) $R/w = 0.3$ (b) $R/w = 0.8$ (c) $R/w = 1.4$ calculated from RO in the case of an open setup with a total power $P = 1$ W, beam waist at the vesicle center $w = 9$ μm, $n_{med} = 1.355$, $n_{vesicle} = 1.37$, $\lambda = 808$ nm. Stress is indicated in concentric rings in Pa. In red, the $\cos^2$ approximation (d): Comparison of the total stretching force projected along the fiber axis from RO calculations and from $\cos^2$ approximation depending on the ratio R/w. Error bars indicate confidence interval of 10%.

ratio R/w. The $\cos^2$ approximation can fit the optical stress profile relatively well for $R/w \sim 0.9$ whereas it tends to overestimate optical stress at high polar angle for high R/w value (see $R/w = 1.4$) and underestimate at high polar angle for low R/w value (see $R/w = 0.3$). Figure S2 also compares the total stretching force projected along the fiber axis calculated from RO and from the $\cos^2$ approximation. It can be seen that the $\cos^2$ approximation gives relatively correct results for an important range of ratio R/w which could explain the good agreement between the proposed deformation model for vesicles and experimental data. However some discrepancies exist at high R/w ratio which could explain the scattered values obtained for bending modulus.

A. Deformation of a vesicle in the optical stretcher

We analyze the deformation of a vesicle according to the quasi-spherical approach described in [5, 6]. In this approach, the shape of the vesicle is parametrized in spherical harmonics as

$$R(\theta,\phi) = R\left(1 + \sum_{l\geq 0}^{l_{max}} \sum_{m=-l}^{l} u_{lm}\mathcal{Y}_{lm}(\theta,\phi)\right), \tag{1}$$

where $\mathcal{Y}_{lm}(\theta,\phi)$ are the normalized spherical harmonic functions and u_{lm} their associated amplitudes. The radius of the vesicle R is given by the constant volume of the vesicle as $V = \frac{4\pi R^3}{3}$. We assume that the total area A of the vesicle is fixed and can be expressed by $A = (4\pi + \Delta)R^2$ where Δ is the dimensionless excess area related to the difference between apparent area and true area. By expanding the geometrical quantities (volume and area) around a sphere, it is straightforward to obtain [6]

$$u_{00} = -\sum_{l\geq 1}^{l_{max}} \sum_{m=-l}^{l} |u_{lm}|^2/\sqrt{4\pi}, \tag{2}$$

and

$$\sum_{l\geq 1}^{l_{max}} \sum_{m=-l}^{l} |u_{lm}|^2 \frac{(l+2)(l-1)}{2} = \Delta, \tag{3}$$

expressing the volume and area constraints respectively. The upper cutoff l_{max} is of order R/d where d is the membrane thickness. For a vesicle with $R \simeq 10 - 50\mu m$, l_{max} is of order 10^4.

The energy induced by the optical trap is taken into account in the total free energy of the vesicle. The shape of the vesicle results then from the minimization of the free energy. The total free energy is the sum of three terms : the bending energy F_κ, a surface energy F_Σ and the stretching energy F_s as

$$F = F_\kappa + F_s + F_\Sigma. \tag{4}$$

Bending energy can be expressed by

$$F_\kappa = \kappa[8\pi + \frac{1}{2}\sum_{l,m} |u_{lm}|^2 (l+2)(l+1)l(l-1) + O(u_{lm}^3)], \tag{5}$$

where κ is the bending rigidity.

The area constraint (3) is taken into account as an area energy such that

$$F_\Sigma = \Sigma \oint dA, \tag{6}$$

where the effective tension Σ of the vesicle is the Lagrangian multiplier associated with the area. We define a dimensionless tension $\tilde{\gamma}$ by $\tilde{\gamma} \equiv \Sigma\ R^2/\kappa$.

To model the stretching energy, it is convenient to use the analytical approximation suggested by *Wottawah et al.* [7] where the stress is approximated by $\sigma(\theta) = \sigma_0 \cos^2(\theta)$. The calculation below can be extended to other analytical functions for the stress as it is always possible to decompose the stress distribution in spherical harmonics and do a

similar development as below. Thus, in the case of $\sigma = \sigma_0 \cos^2(\theta)$, the stretching energy is

$$F_s = -\sigma_0 \oint \cos^2\theta \, [R(\theta,\phi) - R] dA \tag{7}$$

The stress distribution can be decomposed in spherical harmonics to give $\cos^2(\theta) = [\sqrt{16\pi/5}\ \mathcal{Y}_{20} + 1]/3$. So the stretching energy becomes

$$F_s = -(\sigma_0 R^3/3)[\sqrt{4\pi} u_{00} + \sqrt{16\pi/5}\ u_{20}]. \tag{8}$$

We define a dimensionless stress parameter such as $\tilde{f} = \frac{2\sigma_0 R^3}{3\kappa}$. This leads to the expression of the total free energy

$$F = \frac{\kappa}{2} \sum_{l,m} E_l |u_{lm}|^2 - \kappa \tilde{f} \sqrt{4\pi/5} u_{20}, \tag{9}$$

with

$$E_l = (l+2)(l-1)[l(l+1) + \tilde{\gamma} + \tilde{f}/(l+2)(l-1)]. \tag{10}$$

The mean shape of vesicles in the optical stretcher now follows from this energy as there is only one mode with a non-zero mean amplitude which is the elliptical one,

$$\bar{u}_{20} = \frac{\sqrt{4\pi/5}\ \tilde{f}}{24 + 4\tilde{\gamma} + \tilde{f}}, \tag{11}$$

where the bar on any parameter indicates the change due to the optical stretcher relative to the spherical case. Experimentally, $\bar{u}_{20}$ is directly related by equation (1) to the relative major and minor axis strains, ΔM and Δm, respectively, by

$$\bar{u}_{20} = \frac{2}{3}\sqrt{\frac{4\pi}{5}} \left(\frac{\Delta M}{R} - \frac{\Delta m}{R} \right). \tag{12}$$

The area stored in the elliptical mode is, from equations (3) and (11)

$$\bar{\Delta} = 2\bar{u}_{20}^2 = 2\frac{(4\pi/5)\tilde{f}^2}{(24 + 4\tilde{\gamma} + \tilde{f})^2}. \tag{13}$$

The area stored in the fluctuations becomes

$$\Delta_{fl} = \frac{kT}{2\kappa} \sum_{l,m} \frac{(l+2)(l-1)}{E_l} = \frac{kT}{2\kappa} \sum_{l\geq 2} \frac{2l+1}{l(l+1) + \tilde{\gamma} + \tilde{f}/(l+2)(l-1)} \tag{14}$$

$$= \frac{kT}{2\kappa} \ \frac{5}{6 + \tilde{\gamma} + \tilde{f}/4} + \frac{kT}{2\kappa} \sum_{l\geq 3} \frac{2l+1}{l(l+1) + \tilde{\gamma} + \tilde{f}/(l+2)(l-1)}. \tag{15}$$

The total area constraint reads then

$$\Delta = \bar{\Delta} + \Delta_{fl}. \tag{16}$$

This equation is the general equation to calculate the dependence of the effective tension $\tilde{\gamma} = \tilde{\gamma}(\Delta, \kappa, \tilde{f}, l_{max})$ and to deduce the vesicle shape in the optical stretcher.

For vanishing laser amplitude ($\tilde{f} = 0$) the dimensionless initial effective tension $\tilde{\gamma}_0 = \frac{\Sigma_0.R^2}{\kappa}$ (resp. the initial effective tension Σ_0) can be derived analytically from equations (15), and (16) as follows in three regimes [5]

(i) *Tense regime:* For $\Delta << kT/2\kappa$, one obtains

$$\tilde{\gamma}_0 \approx \frac{kT}{2\kappa\Delta} l_{max}^2. \tag{17}$$

For bending moduli between $1-100\ kT$, this corresponds to dimensionless initial effective tension $\tilde{\gamma}_0 >> 10^8$ which gives for a typical radius of 10 μm: $\Sigma_0 >> 10^{-3}$ N/m. In this regime, all N modes share the available excess area [5].

(ii) *Entropic regime:* For $kT/2\kappa << \Delta << (kT/\kappa)\ln l_{max}$, the tension depends exponentially on the excess area

$$\tilde{\gamma}_0 \approx l_{max}^2 e^{-2\kappa\Delta/kT}. \tag{18}$$

This regime corresponds to effective tension between $10^{-7} << \Sigma_0 << 10^{-3}$ N/m for $\kappa \approx 1-100\ kT$ and $R \approx 10\ \mu m$.

(iii) *Prolate regime:* For $(kT/\kappa)\ln l_{max}^2 << \Delta \leq 1$, most of the excess area is stored in the $(l=2)$-modes. The tension approaches the limiting value -6:

$$\tilde{\gamma}_0 \approx -6 + \frac{5}{2}\frac{kT}{\kappa\Delta}. \tag{19}$$

This regime is associated with negative tension indicating that fluctuations are promoted [6].

For non-vanishing laser amplitude, numerical calculations are necessary to solve the area constraint (eq. (16)) when κ, Δ, $\tilde{f}$ and $l_{max} \approx 10^4$ are known [5]. However below, we approximate this equation in some limiting cases in order to discuss the general behavior.

1. *Low peak-stress regime ($\sigma_0 R << 6\Sigma$)*

For low laser power, the applied stress is weak and the tension term is dominant if $4\tilde{\gamma} >> \tilde{f}$ in equations (11,13). This condition is fulfilled in our experiment at small power (see experimental part).

In the low peak stress regime, we can then obtain a simple expression for the deformation $\bar{u}_{20}$

$$\bar{u}_{20} \approx \frac{\sqrt{4\pi/5}\ \tilde{f}}{24 + 4\tilde{\gamma}}, \tag{20}$$

where $\tilde{\gamma}$ is the effective tension of the vesicle that depends implicitly on the stress but should be close to the initial tension $\tilde{\gamma}_0$ as calculated above.

Finally, the mean shape of the vesicle in the optical stretcher is given by

$$\langle R(\theta,\phi)\rangle = \tilde{R} + R\ \bar{u}_{20}\mathcal{Y}_{20}, \tag{21}$$

where $\tilde{R} = R(1 + \langle u_{0,0}\rangle/\sqrt{4\pi})$.

Considering that in first order, $\tilde{R} \approx \tilde{R}(0) + B.\tilde{f}$, the mean shape of the vesicle in first order becomes

$$\langle R(\theta,\phi)\rangle \approx \tilde{R}(0) + [B + \frac{R}{24 + 4\tilde{\gamma}}(3\cos^2\theta - 1)/2]\tilde{f}, \tag{22}$$

where $\tilde{R}(0)$ is the mean radius at zero optical stress and B is a term independent of $\tilde{f}$.

To take into account the total area constraint (eq. 16), we simplify area expressions using the low peak stress approximation. For $4\tilde{\gamma} >> \tilde{f}$, the stress term can be neglected in eq. (15) to give

$$\Delta_{fl} = \frac{kT}{2\kappa}\ \frac{5}{6 + \tilde{\gamma}} + \frac{kT}{2\kappa}\sum_{l\geq 3}\frac{2l+1}{l(l+1) + \tilde{\gamma}}. \tag{23}$$

Replacing the last term by an integral, we obtain after simplification in the case of the entropic regime which corresponds to the regime investigated experimentally

$$\bar{\Delta} = \frac{kT}{2\kappa}\ln\left(\frac{\Sigma}{\Sigma_0}\right) = \frac{kT}{2\kappa}\ln\left(\frac{\tilde{\gamma}}{\tilde{\gamma}_0}\right), \tag{24}$$

where Σ_0 and Σ are the vesicle effective tension (in N/m) for the initial spherical case and the deformed case. This relation is similar to the one developed in [2].

However, the effective tension cannot be rigorously determined by the law of Laplace as presented for the liquid drop model, since fluctuations and bending rigidity modify it [9]. By combining equations (13) and (24), we can eliminate the effective tension of the vesicle in equation (20) and obtain a relation between $\bar{u}_{20}$ and the peak stress σ_0 within this approximation

$$\sigma_0 = \sqrt{\frac{5}{4\pi}}\bar{u}_{20}\left(\frac{36\kappa}{R^3} + \frac{6\Sigma_0}{R}\exp\left(\frac{4\kappa\bar{u}_{20}^2}{kT}\right)\right), \tag{25}$$

where the fitting parameters are κ and Σ_0, respectively the bending modulus and the effective initial tension of the vesicle. Equation (25) is the standard equation that will be tested where $\bar{u}_{20}$ is evaluated experimentally (with eq. 12) and the peak stress σ_0 calculated numerically from experimental parameters.

2. High peak-stress regime

When the stress is increased and becomes large enough ($\tilde{f} \to \infty$), all the excess area is stored in the elliptical mode $l = 2$. The tension in the vesicle, which depends on the applied stress, is also increased. With $\Delta = \bar{\Delta} = 2\bar{u}_{20}^2$ we can estimate the tension from equation (13) to find

$$\tilde{\gamma} \approx (\sqrt{8\pi/5\Delta} - 1)\tilde{f}/4. \tag{26}$$

So in the high peak-stress regime, the effective tension of the vesicle is expected to depend linearly on the peak-stress.

The cross-over between the 'low peak stress' regime and the 'high peak stress' regime is expected to start at a critical stress σ_c defined by

$$\sigma_c \approx \frac{6\Sigma_0}{R\,(\sqrt{\frac{8\pi}{5\Delta}} - 1)}, \tag{27}$$

where the initial tension Σ_0 can be expressed depending on the tension regime (tense, entropic or prolate). Above a critical stress σ_c, the deformation of the vesicle is expected to saturate with $\bar{u}_{20} \to \sqrt{\frac{\Delta}{2}}$ as long as the quasispherical approach is still appropriate. Indeed, in the high peak stress regime, stronger deformations could take place and further effects such as stretching of the membrane might arise which are not studied here.

III. TEMPERATURE IN THE OS: SIMULATION

Wavelength (nm)	808	1064	1480
Absorption coefficient (cm^{-1})	0.019	0.1458	23.2394
ΔT ($\tilde{N}$) for 1 W total power	2.3	15.9	2092.3
Penetration length	$\approx$ 52 cm	$\approx$ 6.9 cm	430 μm

Table S3: Absorption coefficients, penetration lengths and maximum temperature increase in the setup for 1W of total laser power for the various wavelengths used in this work using thermodynamic coefficients of water at 20$\tilde{N}$.

To confirm the estimates of temperature increase with different wavelengths, we computed the increase in temperature inside the setup using COMSOL software (COMSOL MultiPhysics) for the three wavelengths used in our study. A typical temperature diagram is presented in figure S4a where a sketch of the temperature distribution is depicted inside the glass capillary. The calculated increases in temperature are in agreement with previous published results [3] and estimates are summarized in Table S3. In figure S4b, the temperature increase at the center of the trap rescaled by the maximum temperature increase (given in table S3) is presented as a function of the distance d between the fiber and the center of the trap for the case of the open setup (fiber ends are in water). As the penetration length in water is inversely proportional to the absorption coefficient, the increase in temperature at the center of the trap for 1480 nm laser can be tuned by chang-

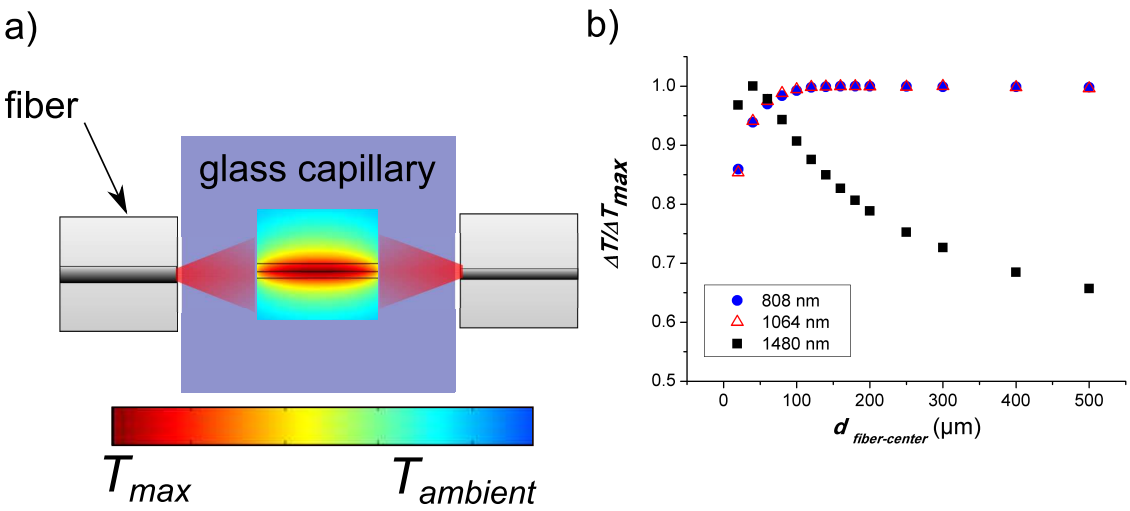

FIG S4: Simulations of temperature increase inside an optical stretcher for different wavelengths. a) Distribution of the temperature inside a microfluidic optical stretcher according to a COMSOL simulation. b) Renormalized increase in temperature $\Delta T/\Delta T_{max}$ as a function of the distance between the fiber ends and at the center of the trap for an open setup (fiber ends are in water). ΔT_{max} is given in Table S3.

ing fiber distance (figure S4b), which is not the case at 808 nm and 1064 nm because penetration lengths are much higher than the size of the microfluidic channel.

IV. DEFORMATION OF DPPC AND DSPC VESICLES WITH A COMBINED 1064/1480 OPTICAL STRETCHER

This figure shows the deformation of DPPC or DSPC vesicles as a function of the 1064 nm total power and 1480 nm total power for about thirty DPPC and DSPC vesicles. The smallest circle corresponds to the absence of deformation ($M = m = R$). Then the bigger the circle is the higher the deformation is. Two transitions lines have been added to enhance a transition between a regime where the deformation is very small and a regime where the deformation is important as explained in the main text.

---

[1] B. Lincoln, F. Wottawah, S. Schinkinger, S. Ebert, and J. Guck, *Methods in Cell Biology* 83 (2007)

[2] K. H. de Haas, C. Blom, D. van den Ende, M. H. G. Duits, and J. Mellema, *Phys. Rev. E* 56, 7132 (1997)

[3] S. Ebert, K. Travis, B. Lincoln, and J. Guck, *Opt. Express* 15, 15493 (2007)

[4] M. Kummrow and W. Helfrich, *Phys. Rev. A* 44, 8356 (1991)

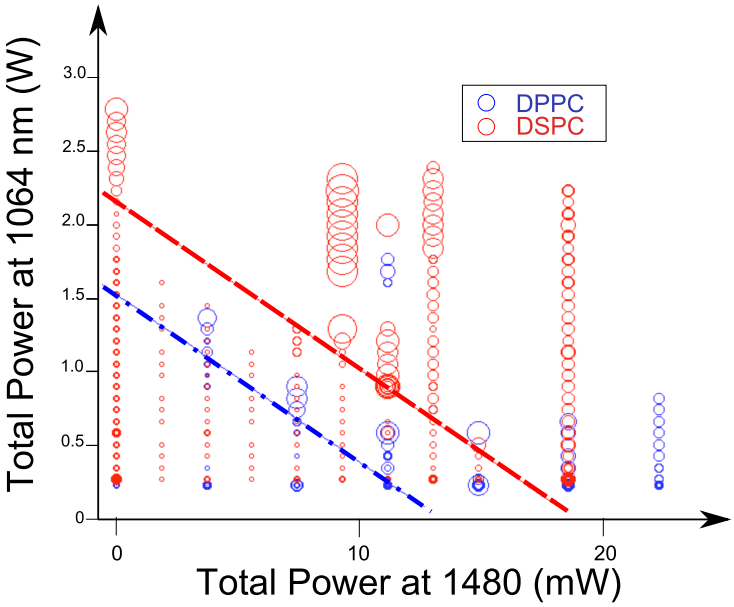

FIG S5: Characterization of the major axis M deformation as a function of the 1064 nm power (total power in W) and the 1480 nm power (total power) inside the 1064/1480 microfluidic optical stretcher for DPPC (blue circle) and DSPC (red circle). The smallest circle with a radius r_0 corresponds to $M = m = R$. Bigger circles with radii $r = (M/m)r_0$ correspond to higher deformations. The two lines are guidelines to indicate the crossover of the melting temperature resulting in a transition between a low deformation regime and a high deformation regime.

[5] U. Seifert, *Eur. Phys. J.B* 8, 405 (1999)

[6] U. Seifert, *Z. Phys. B* 97, 299-309 (1995)

[7] F. Wottawah, S. Schinkinger, B. Lincoln, R. Ananthakrishnan, M. Romeyke, J. Guck, and J. Kas, *Phys. Rev. Lett.* 94, 098103 (2005)

[8] W. Helfrich and R. M. Servuss, *Il Nuovo Cimento* 3, 137 (1984)

[9] V. Vitkova, J. Genova and I. Bivas, *Eur. Biophys. J.* 33, 706 (2004)